Journal of *Marine Science and Engineering*

MDPI

Article

Towards Fuel Consumption Reduction Based on the Optimum Contra-Rotating Propeller

Mina Tadros [1,2,*], Manuel Ventura [1] and C. Guedes Soares [1]

[1] Centre for Marine Technology and Ocean Engineering (CENTEC), Instituto Superior Técnico, Universidade de Lisboa, Av. Rovisco Pais 1, 1049-001 Lisboa, Portugal
[2] Department of Naval Architecture and Marine Engineering, Faculty of Engineering, Alexandria University, Alexandria 21544, Egypt
* Correspondence: mina.tadros@centec.tecnico.ulisboa.pt

Abstract: This paper presents the effect of selecting a contra-rotating propeller (CRP) for a bulk carrier at the engine operating point with minimum fuel consumption, as well as ensuring the safety of the propeller in terms of cavitation and noise. Using a developed optimization model, the geometry of a CRP was selected for different propeller diameters, the same propeller diameter as that of a fixed pitch propeller (FPP) installed on the bulk carrier, and at 90% of the FPP diameter. Additionally, each case was optimized with both no-cup and heavy-cup configurations. In general, the CRP showed better performance than the FPP in terms of efficiency, cavitation, and fuel economy. At the same time, the level of performance was increased when considering the CRP cupping percentage. It was concluded that the CRP can achieve a gain in fuel economy of up to 6.2% in a no-cup configuration when compared to an FPP, and up to 11.7% with a cupped configuration.

Keywords: bulk carrier; contra-rotating propeller; fuel consumption; decarbonization; cavitation; cupping CRP

Citation: Tadros, M.; Ventura, M.; Guedes Soares, C. Towards Fuel Consumption Reduction Based on the Optimum Contra-Rotating Propeller. *J. Mar. Sci. Eng.* **2022**, *10*, 1657. https://doi.org/10.3390/jmse10111657

Academic Editor: Decheng Wan

Received: 4 October 2022
Accepted: 3 November 2022
Published: 4 November 2022

1. Introduction

Due to the need to improve the energy efficiency of ships by reducing fuel consumption and thus carbon dioxide (CO_2) emissions, several solutions have been proposed to minimize the level of energy consumption and achieve the lowest level of exhaust emissions [1]. However, due to the complexity of ships, it has been concluded that no single solution greatly affects the decarbonization process [2,3], and there are many challenges to reducing energy demand even with equipment with lower consumption. However, every retrofitting process from the design or operation concept helps save energy and improve fuel economy.

The propulsion system is the most important system that directly affects the reduction of fuel consumption and exhaust emissions, starting from diesel engines as the prime movers and source of emissions, up to the type of propeller. Therefore, the main interest of industrial companies such as MAN Energy Solutions and Wärtsilä is to improve engine performance by replacing fossil fuels with alternative ones, mainly methanol and ammonia, to be further used in the near future according to strategic plans that present the vision of international organizations [4].

The propulsor, or the propeller, is the second component of the marine propulsion system that directly affects the amount of power transmitted from the engine to the ship hull. The selection of an effective propeller must be carefully performed to ensure high technical efficiency, the required safety during the operation of the ship in calm waters and in severe weather conditions, and to achieve a high level of economic benefit [5,6]. Therefore, optimizing hull forms [7] as well as ship transoms [8] are essential solutions to achieve an appropriate propeller inflow while placing energy-saving devices [9] forward of the propeller, such as pre-swirl ducts [10], pre-swirl fins [11], and vortex generator fins (VGFs) [12], and can be effective solutions for improved energy efficiency.

Besides the previous points, the selection of the marine propeller(s), including the type and the size, coupled with the engine performance, is essential to improve propeller efficiency and reduce fuel consumption [13–15]. This process-based optimization can be performed by comparing several types of propellers from different series and with different propeller shapes, either ducted or non-ducted, to find the optimal fixed pitch propeller (FPP) performance. Additionally, the right choice of the number of blades would be a solution to help reduce fuel consumption [16], especially when reducing the ship speed [17]. The same concept can be considered to achieve a 5% reduction in the fuel consumed, while choosing to utilize a controllable-pitch propeller (CPP) at the engine operating point with minimum fuel consumption compared to only maximizing propeller efficiency [18,19]. Furthermore, increased fuel savings can be achieved by replacing the normal propeller with a cupping type; in addition, an extreme decrease in cavitation values will be observed [20].

The contra-rotating propeller (CRP) is another concept that was developed by Wagner [21] to reduce engine loads and thus increase fuel economy. This concept is based on adding a smaller propeller that rotates in the opposite direction, positioned aft of the main one. As the FPP causes water circulation, placing two different propellers in front of each other assist in neutralizing the water circulation. Therefore, the energy losses from the sideways forces due to water circulation are recovered by the small propeller (aft propeller) and force the water to flow in a horizontal direction parallel to the thrust direction. This system will create a larger thrust force than in the case of a single FPP and increase the propeller efficiency. Figure 1 shows the configuration of a CRP in a model ship.

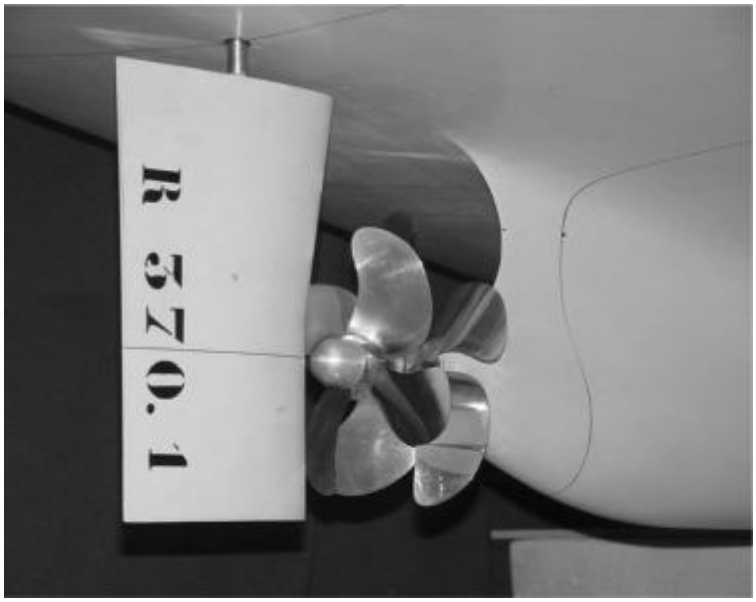

Figure 1. The CRP system at the stern of the model ship [22].

In terms of propeller performance, van Manen and Oosterveld [23] presented the results of the performance of a CRP in open-water conditions compared to a conventional propeller. They predicted higher efficiency with the CRP, accompanied by a reduction in the delivered horsepower (DHP). Min et al. [22] performed model tests of several CRP configurations and concluded that the propulsion efficiency was improved compared to that with a conventional configuration. Koronowicz et al. [24] developed a numerical model to design and generate the two propellers in a 3D mode and computed the hydrodynamic performance of each one for a given ship speed. Additionally, Ghassemi and Taherinasab [25] validated the numerical results from a 3D model developed with real data. They concluded that the hydrodynamic coefficient of the rear propeller was higher than that of the front one due to the wake. The cavitation was improved due to the distribution of loads between the two propellers, and a pressure distribution more

uniform than that obtained with the single propeller was observed. Nouri et al. [26] used optimization procedures coupled with computational fluid dynamics (CFD) techniques to find both propellers' optimal geometries.

In terms of maneuverability, Kayano et al. [27] showed that using a CRP with the tandem arrangement of pod propulsor improves the ship's maneuverability by almost 50% compared to the international standards. Torneman [28] concluded that by using a CRP, the maneuverability as well as the fuel efficiency of a wind farm support vessel (WFSV) on the high seas were increased during transportation from shore to the offshore site.

In terms of operation, Hou et al. [29] used CFD methods to find the operational speed of both propellers. They concluded that the speed of the forward propeller must be higher than that of the rear one to achieve higher propulsive efficiency and avoid any negative effects related to the net torque of the CRP on transverse stability.

In terms of emissions, Minami and Kano [30] showed that the use of a super marine gas turbine (SMGT) coupled with a CRP could reduce CO_2 emissions by 25%, nitrogen oxide (NO_x) emissions by 92%, and sulfur oxide (SO_x) emissions by 73%

From that point of view, this paper contributes to the selection of a coaxial CRP using optimization procedures for a given vessel at the engine operating point with minimum fuel consumption. Based on the literature review, simulations were performed for several propeller diameters. Furthermore, the results were compared to a conventional propeller installed on the ship, as mentioned in the literature, while considering different levels of cupping.

The remainder of this paper is organized as follows. The numerical model used to perform the simulations is presented in Section 2. Next, the computed results and the evaluation of the propeller performance for the design concept are presented in Section 3. Finally, a summary of the main findings and future recommendations are presented in Section 4.

2. Numerical Model

This study considers the selection of a CRP for a bulk carrier of 154 m in length by performing optimization procedures to identify the optimum propeller geometry. The characteristics of the bulk carrier and the main engine installed are given in Table 1.

Table 1. Main characteristics of the bulk carrier.

	Characteristics	Unit	Value
Ship characteristics	Length waterline	m	154.00
	Breadth	m	23.11
	Draft	m	10.00
	Displacement	tonnes	27,690
	Service speed	knots	14.5
	Maximum speed	knots	16.0
	Number of propellers	-	1
	Type of propeller	-	FPP
	Rated power	kW	7140
Engine characteristics	Engine builder	-	MAN Energy Solutions [31]
	Brand name	-	MAN
	Bore	mm	320
	Stroke	mm	440
	Displacement	liters	4954
	Number of cylinders	-	14
	Rated speed	rpm	750
	Rated power	kW	7140

The optimization model used in this study was previously developed by Tadros et al. [20]. In the current paper, the model was adapted to select a contra-rotating propeller

and to compute its performance coupling NavCad software [32], an engine load diagram computed from a 1D engine model [33–35], and a nonlinear optimizer integrated into Matlab [36] using an application programming interface (API) that allows interaction between NavCad and other third parties. A schematic diagram is presented in Figure 2, showing the processing of data through the optimization model. The model was developed to find the optimal propeller parameters and the operational point in order to minimize the fuel consumption of the bulk carrier under different input parameters such as the ship design speed (V_s), number of propeller blades (Z), type of propeller series and the percentage of propeller cupping. The model complies with the limitation of noise and cavitation methods applied.

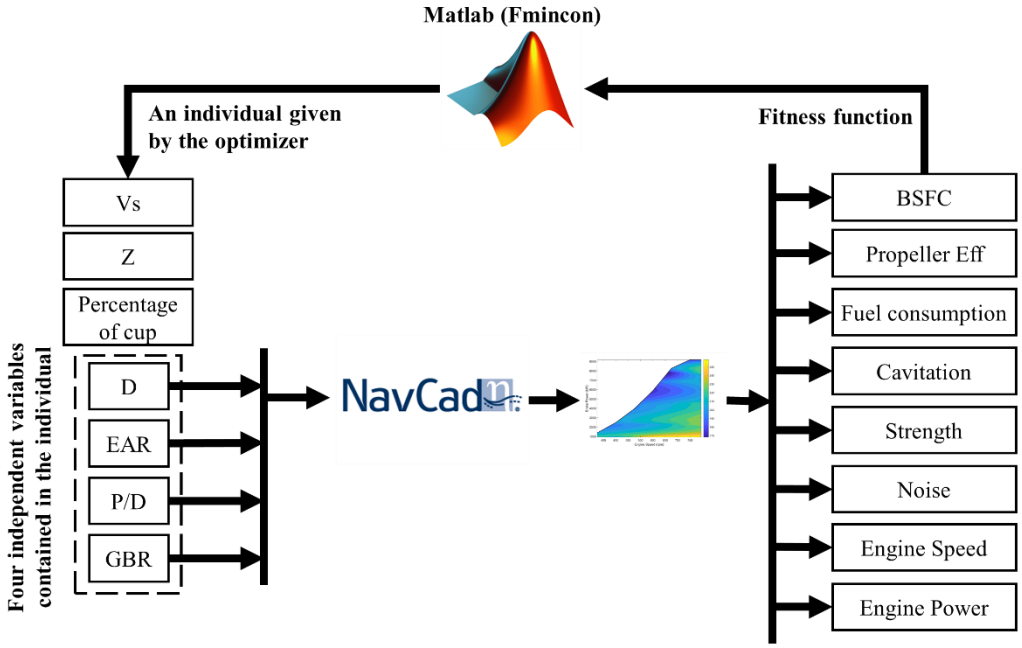

Figure 2. Schematic diagram of the propeller optimization model [20].

In order to perform the simulation, the ship data were exported from the 3D hull and input into NavCad to first compute the ship resistance. Then, the methods presented in [37,38] were used according to the expert ranking tab provided in NavCad to provide the priority of the suitable method among all methods considered in the software, with the total resistance coefficient (C_T) s computed using the following equation:

$$C_T = (1 + k)\, C_F + C_R + C_A \quad (1)$$

where k is the form factor computed based on the equations of the International Towing Tank Conference (ITTC) [39], C_F is the frictional coefficient, C_R is the residuary coefficient, and C_A is the correlation allowance computed according to the recommendations of ITTC 78 [40].

These methods to compute the ship resistance have been validated by comparing the empirical results of several ships with the ones exported from CFD computation, showing good agreement and high accuracy [41]. Figure 3 shows the calculated ship resistance for several ship speeds.

Once the resistance was computed, the propulsive coefficient, including wake fraction (w), thrust deduction factor (t) and relative rotative efficiency (η_{RR}), were estimated using the methods presented in [37,42]. Then, the propeller geometry and gearbox ratio were computed based on the defined propeller series (Wageningen B-series [43] was used in this study), as well as the efficiencies of the propeller shaft and gearbox.

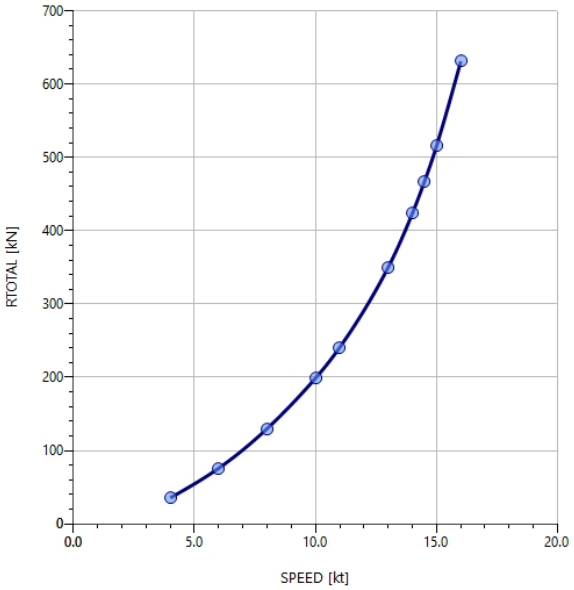

Figure 3. Total ship resistance at different speeds.

The optimization procedure started by defining the initial conditions of propeller geometry, including propeller diameter (D), expanded area ratio (EAR), pitch diameter ratio (P/D) and gearbox ratio (GBR). All of this information was processed in NavCad, and the propeller's performance was computed. Then, the data were exported and passed through the engine load diagram using interpolation to find the interaction between engine and propeller performance. The engine performance at this point could be computed by estimating the brake-specific fuel consumption (BSFC) and the different exhaust emissions (CO_2, NO_x and SO_x). After that, the fuel consumption (FC) in liters per nautical mile was computed using the following equation:

$$FC_{l/nm} = \frac{BSFC \times P_B \times 1000}{\rho_{fuel} \times V_S} \quad (2)$$

where P_B is the brake power, and ρ_{fuel} is the fuel density.

The FC, as the study's main objective, and the different constraints, including cavitation, noise and effective speed-power area inside the engine load diagram presented as penalty functions, were implemented in a fitness function and evaluated using the nonlinear optimizer. More information about the detailed fitness function presented in the following equation can be found in [16]. Then, the process of optimization was repeated until the stopping criteria were met, as shown in Figure 4.

$$Fitness\ Function = FC_{l/nm} + R\sum_{i=1}^{j} max(g_i(x), 0) \quad (3)$$

where R is a constant, g is the penalty function, and j is the number of constraints.

The contra-rotating propeller performance developed in NavCad can be adapted to consider any type of propeller series. At the same time, some corrections have been applied using empirical formulas based on propeller performance in [23,44,45], comparing the FPP to the CRP. Therefore, it is a simplified model that can predict the performance of the CRPs with the definition of the forward propeller only.

This model divides equally the thrust and torque of the total propulsor in half between the blade rows and has lower blade loading than without the other blade row. It considers the increased induced velocity that manifests as a reduction of thrust coefficient (K_T) and torque coefficient (K_Q). Additionally, the recovery of rotational losses manifests as a reduction in propeller torque for the after-blade row, thus increasing the relative

rotative efficiency, which is a measure of the torque. Therefore, based on the propeller model test and self-propulsion tests described in the previous references, some internal corrections in NavCad were applied, without user interaction, to compute the corrected open-water propeller efficiency (η_o), hull efficiency (η_H), and relative rotative efficiency η_{RR} [32] compared to a single FPP. As this model is based on a single propeller, the computed thrust and torque coefficient were for the total CRP unit, while the cavitation parameters were for the forward propeller only.

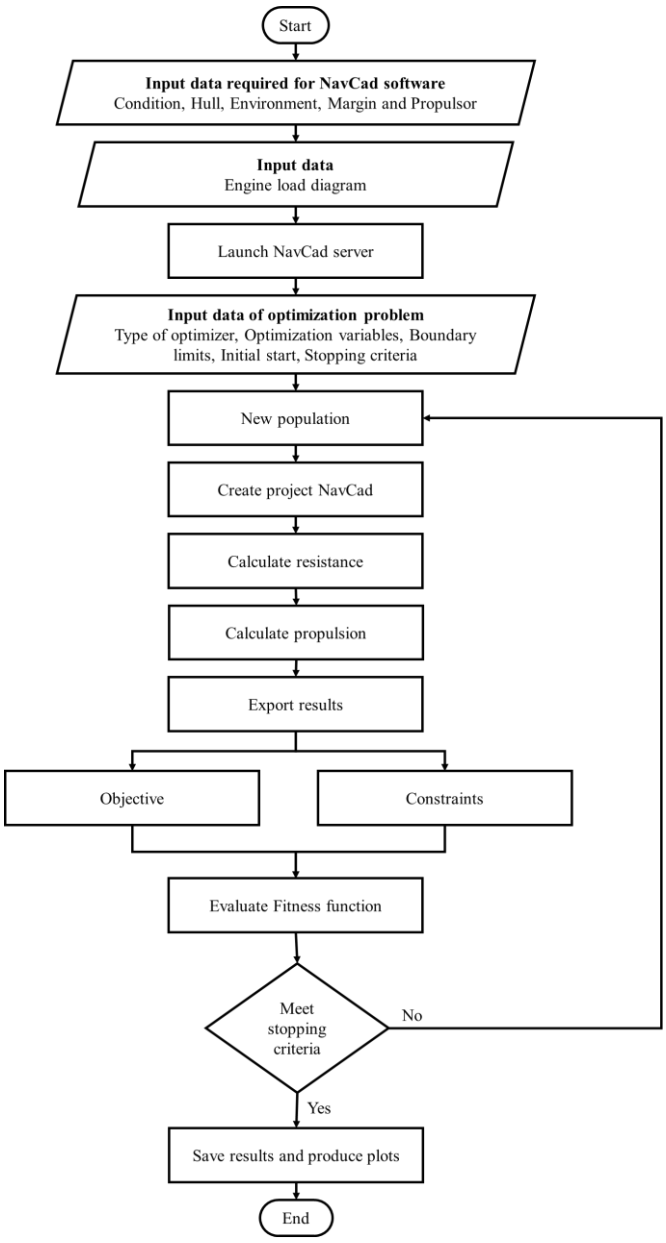

Figure 4. Schematic diagram of optimization tool in calm water.

3. Results and Discussion

After establishing the numerical model, the propeller type, CRP, was selected to perform the optimization procedure. Different upper boundary conditions of propeller diameter were selected to compare the selected CRP with the FPP. The first case was for an upper boundary equal to the FPP (6 m), while the second one equaled 90% of the diameter of the FPP (5.4 m) compared to the propeller mentioned by van Lammeren et al. [46]. Then, each propeller was simulated in two cases; no cup and a heavy cup. All simulations were

performed for a five-blade propeller at a 14.5 knot designed speed. The results are presented in normalized data in Figures 5 and 6, while the real data are presented in Table A1 in Appendix A.

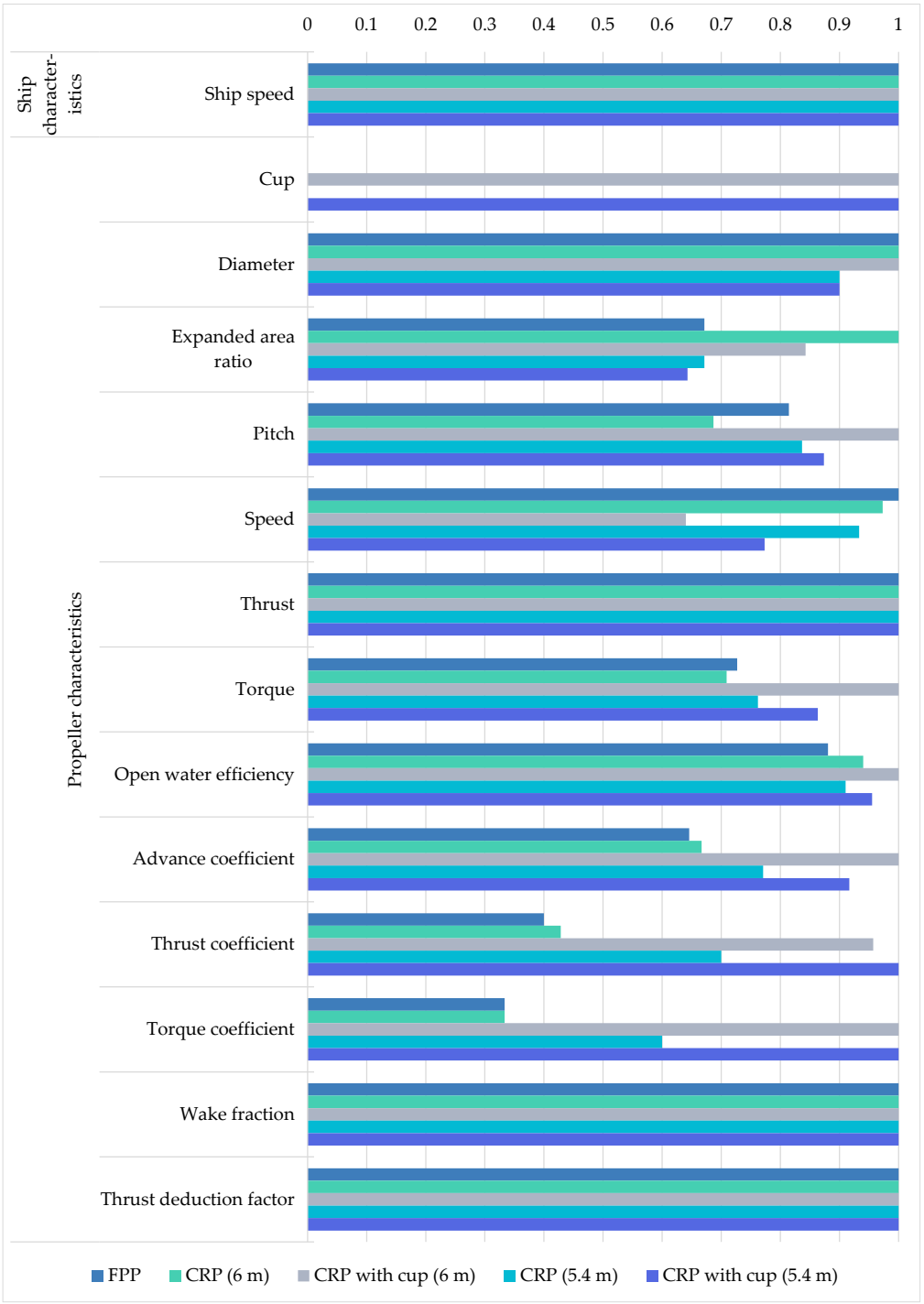

Figure 5. Normalized propeller characteristics for different configurations.

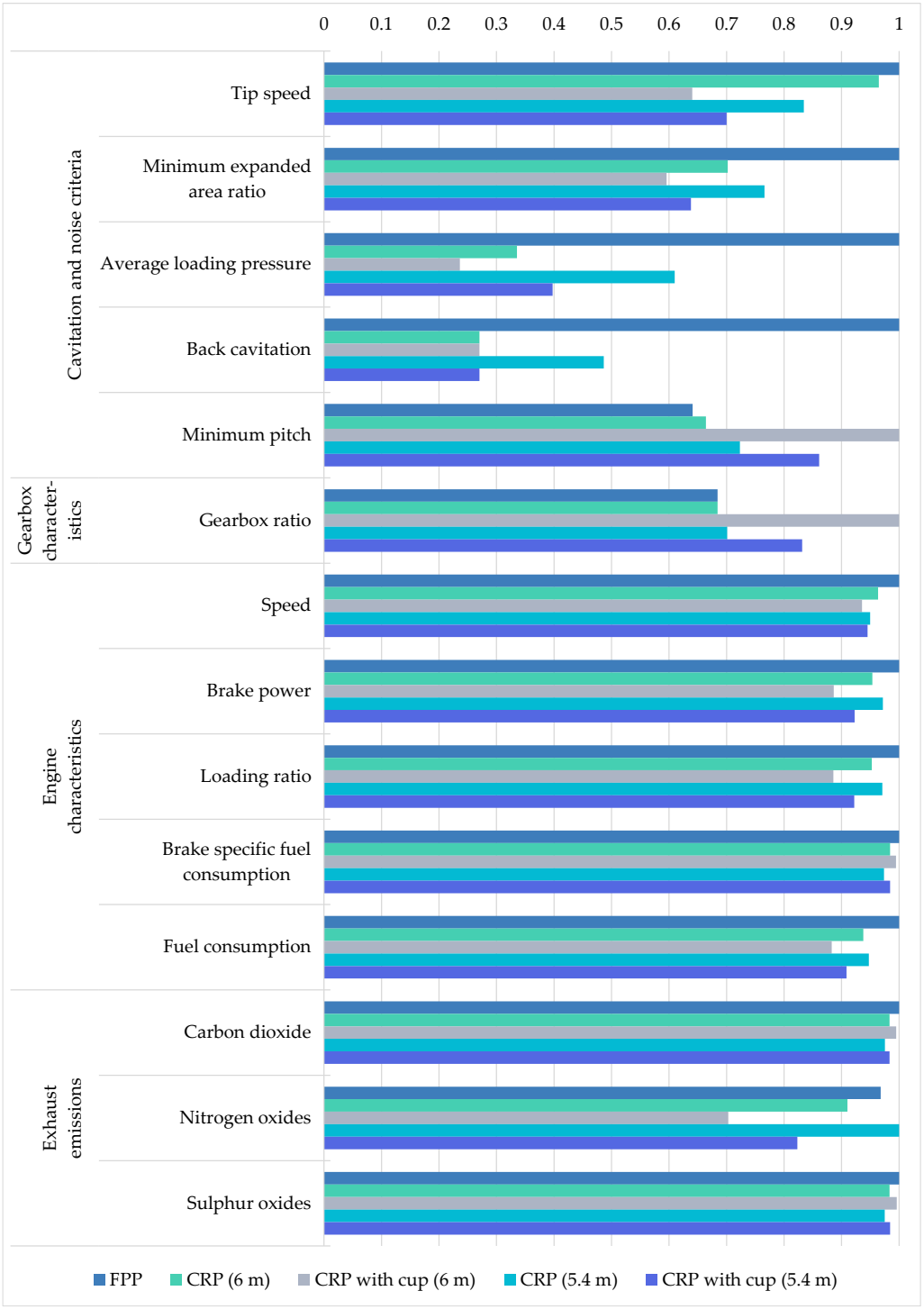

Figure 6. Normalized cavitation criteria, gearbox and engine characteristics and exhaust emissions for different configurations.

After that, the optimization procedures were performed, and the propeller geometry and the operational point were selected to minimize fuel consumption. The model complied with the limitations of the different criteria of cavitation that were defined as model constraints: (1) minimum EAR [43], where the computed EAR must be greater than or equal to minimum EAR based on the Keller method, (2) average loading pressure [47] computed on the basis of the Burrill chart, with values that cannot exceed 65 kPa, (3) the average predicted back cavitation percentage [48], generated from the high power that cannot be handled due to lower blade area, and that cannot exceed 15%, and (4) minimum

pitch to avoid face cavitation [49], where the lower angle of attack causes the blade to generate lift on both blade sides, leading to face cavitation; therefore, the propeller pitch must be greater or equal to the value of the minimum pitch.

Further, the tip speed limitation [32] and minimum blade thickness [43] were verified. The propeller diameter for each case was selected at the upper boundary of the defined parameter. Then, the other parameters, such as EAR and pitch, were selected accordingly by considering the cavitation criteria.

In contrast, the GBR was selected such that the propeller speed did not exceed the level of noise as well as the operating range defined in accordance with the engine load diagram, where the engine could operate smoothly with a high combustion process. All of the selected propellers produced the same thrust required to operate the ship at the designed speed. It was found that the open water efficiency in the case of CRP was increased relative to the FPP and achieved a further increment in the case of a cupping propeller. In addition, the larger diameter selected, the higher the efficiencies achieved relative to the FPP.

The advance coefficient (J_A) was increased in the cases of cupping propellers, where there was a reduction in propeller speed accompanied by an increase in K_T and K_Q. However, there were no changes in the wake fraction and thrust deduction factor values in the five different cases, as confirmed in some studies, such as in [50,51].

Due to the reduction in propeller speed, the tip speed was reduced in the case of CRP and achieved an increment in speed when the propeller was cupped by 33% in the case of a 6 m propeller and 16% in the case of a 5.4 m propeller. The EAR was always greater than the minimum EAR to avoid cavitation, and the minimum EAR in the CRP was smaller than that of the FPP by 30%, while the minimum EAR was reduced in the case of a cupping propeller compared to a normal CRP, by 15% and 17%, respectively, in the case of 6 and 5.4 m propellers, because the propeller was operating at a higher pitch, and therefore, the pressure on the blades was reduced. The same concept applied when computing the average loading pressure and back cavitation criteria, where the first criterion was reduced by 76% compared to the FPP, and the second criterion was reduced by 73% compared to the FPP.

The GBR was computed as a ratio between the propeller and engine speeds, and some increase was achieved in the case of a 6 m propeller with a heavy cup, because the propeller speed was lower.

The engine speed was reduced in the case of a CRP because it could produce the same amount of thrust at lower speeds. Additionally, the brake power was reduced by 3 to 5% compared to that of the FPP. By considering the percentage of cupping, the CRP could operate at speeds 5 to 7% lower than those of an FPP.

There were no significant differences in BSFC for all cases, but because of the lower brake power, fuel consumption was reduced. The no-cup CRP could reduce fuel consumption, by 6.2% in the case of a 6 m propeller and 5.2% in the case of a 5.4 m propeller, compared to an FPP. Moreover, with a cupping propeller, fuel consumption was significantly reduced, by 11.7% in the case of a 6 m and 9.2% in the case of a 5.4 m propeller, compared to an FPP. As fuel consumption was reduced, the different exhaust emissions were also reduced, to levels corresponding to the reduced levels of fuel consumption.

4. Conclusions

This paper presents the selection of CRPs with different propeller diameters corresponding to the ship selected and the cases presented in a literature review. Further, the cupping percentage was considered to select a more effective propeller.

The propeller was selected for the designed speed using a developed optimization model coupling NavCad, an optimizer in the Matlab environment, and a surrogate model presenting the engine performance. The optimization model was able to select the propeller geometry and the operational point in order to minimize fuel consumption. Additionally, the model complied with stipulated limitations on cavitation and noise.

The propeller selection process is very fast, as it depends on the propeller series to perform a preliminary investigation in propeller selection for the concept of ship design. With some simplifications, the geometry of the forward propeller was selected, while the model was able to select the performance of the CRP unit.

In terms of propeller performance, it was found that the performance of the CRP unit, in general, was higher than that of an FPP and increased when the cupping percentage was considered.

In terms of cavitation and noise, a CRP unit is more resistant to cavitation, as the amount of thrust is divided between the two rows; therefore, the probability of the occurrence of cavitation was reduced when the different cavitation criteria were evaluated. In addition, the noise level was reduced, as the tip speed was reduced in comparison with that of an FPP.

In terms of fuel consumption, the CRP showed better fuel economy, as the propeller was operated at a lower loading ratio than that of an FPP. This percentage was increased when the model considered a cupping CRP. Compared to an FPP, a no-cup CRP unit could achieve a reduction in fuel consumption by up to 6.2%, while a cupped CRP could achieve a reduction of up to 11.7%.

This work presents a preliminary estimation of the performance of a CRP in comparison with an FPP, with and without cupping. More investigations can be performed for other propeller series that are able to reach higher values of fuel savings and propeller performance than the B series. Furthermore, it would be interesting to consider CFD computations for the same propeller selected to validate the calculation of the wake field, which could provide additional improvements to the wake calculation using empirical formulas.

Author Contributions: The study concept was developed by M.T. The analysis was performed by M.T., and the original draft manuscript was written by M.T., M.V. and C.G.S. All authors have read and agreed to the published version of the manuscript.

Funding: This work was performed within the scope of the Strategic Research Plan of the Centre for Marine Technology and Ocean Engineering (CENTEC), which is financed by the Portuguese Foundation for Science and Technology (Fundação para a Ciência e Tecnologia-FCT) under contract UIDB/UIDP/00134/2020.

Institutional Review Board Statement: Not applicable.

Informed Consent Statement: Not applicable.

Data Availability Statement: The data presented in this study are available on request from the corresponding author.

Conflicts of Interest: The authors declare no conflict of interest.

Abbreviations

η_H	Hull efficiency
η_o	Open-water propeller efficiency
η_{RR}	Relative-rotative efficiency
3D	Three dimensional
API	Application programming interface
BSFC	Brake-specific fuel consumption
C_A	Correlation allowance
CAV_{AVG}	Back cavitation
C_F	Frictional coefficient
CFD	Computational fluid dynamics
CO_2	Carbon dioxide
CPP	Controllable pitch propeller
C_R	Residuary coefficient
CRP	Contra-rotating propeller
C_T	Total resistance coefficient
D	Propeller diameter

DHP	Delivered horsepower
EAR	Expanded area ratio
EAR_{min}	Minimum expanded area ratio
FC	Fuel consumption
FPP	Fixed pitch propeller
g	Penalty function
GBR	Gearbox ratio
ITTC	International Towing Tank Conference
j	Number of constraints
J_A	Advance coefficient
k	Form factor
K_Q	Torque coefficient
K_T	Thrust coefficient
LR	Loading ratio
N	Propeller speed
NO_x	Nitrogen oxides
P/D	Pitch diameter ratio
P_B	Brake power
P_{FC}	Minimum pitch
PRESS	Average loading pressure
Q	Propeller torque
R	Constant
RPM	Engine speed
SMGT	Super marine gas turbine
SO_x	Sulphur oxides
t	Thrust deduction factor
T	Propeller thrust
VGFs	Vortex generator fins
V_s	Ship design speed
V_{tip}	Tip speed
w	Wake fraction
WFSV	Wind farm support vessel
Z	Number of propeller blades
ρ_{fuel}	Fuel density

Appendix A

Table A1. Optimum results for different configurations.

Main Characteristics	Parameters	Symbol	Unit					
Propeller type			[-]	FPP	CRP (6 m)	CRP with cup (6 m)	CRP (5.4 m)	CRP with cup (5.4 m)
Ship characteristics	Ship speed	V_s	[kn]	14.5	14.5	14.5	14.5	14.5
Propeller characteristics	Series	[-]	[-]	Wageningen B-series				
	Cup	[-]	[%]	0.00	0.00	1.50	0.00	1.50
	Diameter	D	[m]	6.00	6.00	6.00	5.40	5.40
	Expanded area ratio	EAR	[-]	0.47	0.70	0.59	0.47	0.45
	Pitch	P	[m]	6.58	5.55	8.08	6.76	7.06
	Speed	N	[RPM]	75	73	48	70	58
	Thrust	T	[kN]	576.49	576.49	576.49	576.49	576.49
	Torque	Q	[kN·m]	573.30	559.20	788.50	600.90	680.70
	Open water efficiency	η_o	[%]	59	63	67	61	64
	Advance coefficient	J_A	[-]	0.62	0.64	0.96	0.74	0.88
	Thrust coefficient	K_T	[-]	0.28	0.30	0.67	0.49	0.70
	Torque coefficient	K_Q	[-]	0.05	0.05	0.15	0.09	0.15
	Wake fraction	w	[-]	0.38	0.38	0.38	0.38	0.38
	Thrust deduction factor	t	[-]	0.19	0.19	0.19	0.19	0.19

Table A1. *Cont.*

Main Characteristics	Parameters	Symbol	Unit					
Cavitation and noise criteria	Tip Speed	V_{tip}	[m/s]	23.61	22.78	15.12	19.70	16.53
	Minimum expanded area ratio	EAR_{min}	[-]	0.47	0.33	0.28	0.36	0.30
	Average loading pressure	PRESS	[kPa]	43.56	14.62	10.30	26.57	17.32
	Back cavitation	CAV_{AVG}	[%]	7.40	2.00	2.00	3.60	2.00
	Minimum pitch	P_{FC}	[m]	4.98	5.16	7.77	5.62	6.69
Gearbox characteristics	Gearbox ratio	GBR	[-]	9.50	9.50	13.88	9.73	11.54
Engine characteristics	Speed	RPM	[RPM]	714	688	668	678	675
	Brake power	P_B	[kW]	4682	4465	4151	4551	4321
	Loading ratio	LR	[%]	65.6	62.5	58.1	63.7	60.5
	BSFC	BSFC	[g/kW·h]	192	189	191	187	189
	Fuel consumption	FC	[l/nm]	74.17	69.56	65.48	70.28	67.38
Exhaust emissions	Carbon dioxide	CO_2	[g/kW·h]	608	598	605	593	598
	Nitrogen oxides	NO_x	[g/kW·h]	6.68	6.28	4.85	6.90	5.68
	Sulphur oxides	SO_x	[g/kW·h]	9.59	9.43	9.55	9.35	9.44

References

1. Bouman, E.A.; Lindstad, E.; Rialland, A.I.; Strømman, A.H. State-of-the-art technologies, measures, and potential for reducing GHG emissions from shipping—A review. *Transp. Res. D Transp. Environ.* **2017**, *52*, 408–421. [CrossRef]
2. Green Ship of the Future. 2019 Retrofit Project. Available online: https://greenship.org/project/2019-retrofit-series/ (accessed on 8 December 2021).
3. Karatuğ, Ç.; Arslanoğlu, Y.; Guedes Soares, C. Evaluation of decarbonization strategies for existing ships. In *Trends in Maritime Technology and Engineering*; Guedes Soares, C., Santos, T.A., Eds.; Taylor & Francis Group: London, UK, 2022; pp. 45–54.
4. DNV. *Maritime Forecast to 2050: Energy Transition Outlook 2020*; DNV: Bærum, Norway, 2020.
5. Tadros, M.; Vettor, R.; Ventura, M.; Guedes Soares, C. Effect of different speed reduction strategies on ship fuel consumption in realistic weather conditions. In *Trends in Maritime Technology and Engineering*; Guedes Soares, C., Santos, T.A., Eds.; Taylor & Francis Group: London, UK, 2022; pp. 553–561.
6. Vettor, R.; Tadros, M.; Ventura, M.; Guedes Soares, C. Route planning of a fishing vessel in coastal waters with fuel consumption restraint. In *Maritime Technology and Engineering 3*; Guedes Soares, C., Santos, T.A., Eds.; Taylor & Francis Group: London, UK, 2016; pp. 167–173.
7. Ventura, M. Ship dimensioning in the initial design. In *Developments in Maritime Transportation and Exploitation of Sea Resources*; Guedes Soares, C., López Peña, F., Eds.; Taylor & Francis Group: London, UK, 2014; pp. 531–539.
8. Feng, Y.; el Moctar, O.; Schellin, T.E. Parametric Hull Form Optimization of Containerships for Minimum Resistance in Calm Water and in Waves. *J. Mar. Sci. Appl.* **2021**, *20*, 670–693. [CrossRef]
9. Stark, C.; Xu, Y.; Zhang, M.; Yuan, Z.; Tao, L.; Shi, W. Study on Applicability of Energy-Saving Devices to Hydrogen Fuel Cell-Powered Ships. *J. Mar. Sci. Eng.* **2022**, *10*, 388. [CrossRef]
10. Andersson, J.; Shiri, A.A.; Bensow, R.E.; Yixing, J.; Chengsheng, W.; Gengyao, Q.; Deng, G.; Queutey, P.; Xing-Kaeding, Y.; Horn, P.; et al. Ship-scale CFD benchmark study of a pre-swirl duct on KVLCC2. *Appl. Ocean Res.* **2022**, *123*, 103134. [CrossRef]
11. Gaggero, S.; Martinelli, M. Pre-swirl fins design for improved propulsive performances: Application to fast twin-screw passenger ships. *J. Ocean Eng. Mar. Energy* **2022**. [CrossRef]
12. Seol, H. Virtue and Function. *The Naval Architect*. Available online: https://www.rina.org.uk/Virtue_and_function.html (accessed on 8 September 2022).
13. Tadros, M.; Ventura, M.; Guedes Soares, C. Design of Propeller Series Optimizing Fuel Consumption and Propeller Efficiency. *J. Mar. Sci. Eng.* **2021**, *9*, 1226. [CrossRef]
14. Nelson, M.; Temple, D.W.; Hwang, J.T.; Young, Y.L.; Martins, J.R.R.A.; Collette, M. Simultaneous optimization of propeller–hull systems to minimize lifetime fuel consumption. *Appl. Ocean Res.* **2013**, *43*, 46–52. [CrossRef]
15. Tadros, M.; Ventura, M.; Guedes Soares, C. Optimum design of a container ship's propeller from Wageningen B-series at the minimum BSFC. In *Sustainable Development and Innovations in Marine Technologies*; Georgiev, P., Guedes Soares, C., Eds.; Taylor & Francis Group: London, UK, 2020; pp. 269–274.
16. Tadros, M.; Vettor, R.; Ventura, M.; Guedes Soares, C. Coupled Engine-Propeller Selection Procedure to Minimize Fuel Consumption at a Specified Speed. *J. Mar. Sci. Eng.* **2021**, *9*, 59. [CrossRef]
17. Jaurola, M.; Hedin, A.; Tikkanen, S.; Huhtala, K. A TOpti simulation for finding fuel saving by optimising propulsion control and power management. *J. Mar. Sci. Technol.* **2020**, *25*, 411–425. [CrossRef]
18. Tadros, M.; Ventura, M.; Guedes Soares, C. Optimization procedures for a twin controllable pitch propeller of a ROPAX ship at minimum fuel consumption. *J. Mar. Eng. Technol.* **2022**. [CrossRef]

19. Makino, H.; Umeda, N.; Ohtsuka, T.; Ikejima, S.; Sekiguchi, H.; Tanizawa, K.; Suzuki, J.; Fukazawa, M. Energy savings for ship propulsion in waves based on real-time optimal control of propeller pitch and electric propulsion. *J. Mar. Sci. Technol.* **2017**, *22*, 546–558. [CrossRef]
20. Tadros, M.; Vettor, R.; Ventura, M.; Guedes Soares, C. Effect of propeller cup on the reduction of fuel consumption in realistic weather conditions. *J. Mar. Sci. Eng.* **2022**, *10*, 1039. [CrossRef]
21. Wagner, R. Rückblick und Ausblick auf die Entwicklung des Contrapropellers. In *Jahrbuch der Schiffbautechnischen Gesellschaft: 30. Band*; Springer: Berlin/Heidelberg, Germany, 1929; pp. 195–256.
22. Min, K.-S.; Chang, B.-J.; Seo, H.-W. Study on the Contra-Rotating Propeller system design and full-scale performance prediction method. *Int. J. Nav. Arch. Ocean Eng.* **2009**, *1*, 29–38. [CrossRef]
23. van Manen, J.D.; Oosterveld, M.W.C. Model Tests on Contra-Rotating Propellers. *Int. Shipbuild. Prog.* **1969**, *15*, 401–417. [CrossRef]
24. Koronowicz, T.; Krzemianowski, Z.; Tuszkowska, T.; Szantyr, J. A complete design of contra-rotating propellers using the new computer system. *Pol. Marit. Res.* **2010**, *17*, 14–24. [CrossRef]
25. Ghassemi, H.; Taherinasab, M. Numerical calculations of the hydrodynamic performance of the contra-rotating propeller (CRP) for high speed vehicle. *Pol. Marit. Res.* **2013**, *20*, 13–20. [CrossRef]
26. Nouri, N.M.; Mohammadi, S.; Zarezadeh, M. Optimization of a marine contra-rotating propellers set. *Ocean Eng.* **2018**, *167*, 397–404. [CrossRef]
27. Kayano, J.; Haraguchi, T.; Tsukada, Y.; Kano, T. On the ship maneuverability of tandem arrangement CRP pod propulsion system. In *Maritime Transportation and Exploitation of Ocean and Coastal Resources*; Guedes Soares, C., Garbatov, Y., Fonseca, N., Eds.; Taylor and Fransis: London, UK, 2005; pp. 189–193.
28. Torneman, G. Multiple pod units for efficient vessel handling in wind farm operations. In *Design & Operation of Offshore Wind Farm Support Vessels*; Royal Institution of Naval Architects: London, UK, 2015.
29. Hou, L.; Yin, L.; Hu, A.; Chang, X.; Lin, Y.; Wang, S. Optimal matching investigation of marine contra-rotating propellers for energy consumption minimization. *J. Mar. Sci. Technol.* **2021**, *26*, 1184–1197. [CrossRef]
30. Minami, Y.; Kano, T. Evaluation of the emissions from the super eco-ship and the corresponding conventional ship. In *Maritime Transportation and Exploitation of Ocean and Coastal Resources*; Guedes Soares, C., Garbatov, Y., Fonseca, N., Eds.; Taylor and Fransis: London, UK, 2005; pp. 1721–1727.
31. MAN Diesel & Turbo. *32/44CR Project Guide—Marine Four-Stroke Diesel Engines Compliant with IMO Tier II*; MAN Diesel & Turbo: Augsburg, Germany, 2017.
32. HydroComp. NavCad: Reliable and Confident Performance Prediction. *HydroComp Inc.* Available online: https://www.hydrocompinc.com/solutions/navcad/ (accessed on 30 January 2019).
33. Tadros, M.; Ventura, M.; Guedes Soares, C. Surrogate models of the performance and exhaust emissions of marine diesel engines for ship conceptual design. In *Maritime Transportation and Harvesting of Sea Resources*; Guedes Soares, C., Teixeira, A.P., Eds.; Taylor & Francis Group: London, UK, 2018; pp. 105–112.
34. Tadros, M.; Ventura, M.; Guedes Soares, C. Optimization procedure to minimize fuel consumption of a four-stroke marine turbocharged diesel engine. *Energy* **2019**, *168*, 897–908. [CrossRef]
35. Tadros, M.; Ventura, M.; Guedes Soares, C. Simulation of the performance of marine Genset based on double-Wiebe function. In *Sustainable Development and Innovations in Marine Technologies*; Georgiev, P., Guedes Soares, C., Eds.; Taylor & Francis Group: London, UK, 2020; pp. 292–299.
36. The MathWorks Inc. Fmincon. Available online: https://www.mathworks.com/help/optim/ug/fmincon.html (accessed on 2 June 2017).
37. Holtrop, J. A statistical re-analysis of resistance and propulsion data. *Int. Shipbuild. Prog.* **1984**, *31*, 272–276.
38. Holtrop, J. A Statistical Resistance Prediction Method With a Speed Dependent Form Factor. In *Proceedings of Scientific and Methodological Seminar on Ship Hydrodynamics (SMSSH'88)*; Bulgarian Ship Hydrodynamics Centre: Varna, Bulgaria, 1988; pp. 1–7.
39. ITTC. Skin Friction and Turbulence Stimulation. In Proceedings of the 8th ITTC, Madrid, Spain, 15–23 September 1957.
40. ITTC. 1978 ITTC Performance Prediction Method. In Proceedings of the 28th ITTC, Wuxi, China, 27 November–2 December 2017.
41. Islam, H.; Ventura, M.; Guedes Soares, C.; Tadros, M.; Abdelwahab, H.S. Comparison between empirical and CFD based methods for ship resistance and power prediction. In *Trends in Maritime Technology and Engineering*; Guedes Soares, C., Santos, T.A., Eds.; Taylor & Francis Group: London, UK, 2022; pp. 347–357.
42. Holtrop, J.; Mennen, G.G.J. An approximate power prediction method. *Int. Shipbuild. Prog.* **1982**, *29*, 166–170. [CrossRef]
43. Oosterveld, M.; Van Oossanen, P. Further computer-analyzed data of the Wageningen B-screw series. *Int. Shipbuild. Prog.* **1975**, *22*, 251–262. [CrossRef]
44. Lindgren, H.; Johnsson, C.-A.; Dyne, G. Studies of the Application of Ducted and Contrarotating Propellers on Merchant Ships. In *Seventh ONR Symposium on Naval Hydrodynamics*; Cooper, R.D., Doroff, S.W., Eds.; Office of Naval Research: Arlington, VA, USA, 1968.
45. Bjarne, E. Systematic Studies of Contra-rotating Propellers for Merchant Ships. In *Proceedings International Maritime and Shipping Conference (IMAS)*; Institute of Marine Engineers: London, UK, 1973.
46. van Lammeren, W.P.A.; van Manen, J.D.; Oosterveld, M.W.C. The Wageningen B-screw series. *Trans. SNAME* **1969**, *77*, 269–317.
47. Burrill, L.C.; Emerson, A. Propeller cavitation: Further tests on 16in. propeller models in the King's College cavitation tunnel. *Int. Shipbuild. Prog.* **1963**, *10*, 119–131. [CrossRef]

48. Blount, D.L.; Fox, D.L. Design Considerations for Propellers in a Cavitating Environment. *Mar. Technol.* **1978**, *15*, 144–178. [CrossRef]
49. MacPherson, D.M. Reliable Propeller Selection for Work Boats and Pleasure Craft: Techniques Using a Personal Computer. In *SNAME Fourth Biennial Power Boat Symposium*; SNAME: Alexandria, VA, USA, 1991.
50. Sasaki, N.; Kuroda, M.; Fujisawa, J.; Imoto, T.; Masaharu, S. On the Model Tests and Design Method of Hybrid CRP Podded Propulsion System of a Feeder Container Ship. In *Proceedings of the First International Symposium on Marine Propulsors (SMP'09)*; Koushan, K., Steen, S., Eds.; Norwegian Marine Technology Research Institute (MARINTEK): Trondheim, Norway, 2009.
51. Sasaki, N.; Murakami, M.; Nozawa, K.; Soejima, S.; Shikaki, A.; Aono, T. Design system for optimum contra-rotating propellers. *J. Mar. Sci. Technol.* **1998**, *3*, 3–21. [CrossRef]